Design and Implementation of a QCL-based QEPAS Sensor Platform for Trace Gas Detection

Wenzhe Jiang, Advisor Frank Tittel

Abstract—**QEPAS is a rapidly developing photoacoustic spectroscopy technique for sensitive trace gas detection in a small sample volume. A QCL-based QEPAS sensor platform was designed and implemented. Four target chemical species were investigated with a QEPAS sensor platform: sulfur dioxide (SO_2), carbon monoxide (CO), and nitrous/methane oxide (N2O/CH4). A novel dual filter structure was employed to remove optical noise induced by the QCL output beam shape in the case of a SO_2 measurement. The 1σ minimum detection limit of CO reached 2ppbv with 1 second time resolution. The N_2O and CH_4 were measured simultaneously with 16ppbv detection limit for N_2O and 60ppbv detection limit for CH_4, which proved the potential of the QEPAS sensor platform to detect multiple gas species simultaneously.**

Index Terms—**Quantum Cascade Laser (QCL), Quartz Enhanced Photo Acoustic Spectroscopy (QEPAS), cascade filter, micro-resonator (mR), wavelength modulation spectroscopy**

I. INTRODUCTION

The development of trace gas detection techniques and the design of robust and compact gas sensors are of considerable interest in applications such as gas impurity measurement, environmental monitoring, industrial process control and medical diagnostics [1-7]. Laser photoacoustic spectroscopy (PAS) is a widely used technology in trace gas detection applications, which has such merits as wide dynamic range, simplicity of use, high selectivity and sensitivity [8-12]. Photoacoustic spectroscopy is based on the photoacoustic effect which was first discovered by Alexander Graham Bell in 1880 [13]. When light is absorbed by a sample, the absorbed energy is transformed to heat energy by non-radiative processes, which results in an increase of the localized temperature and pressure in the sample. Therefore the absorption of modulated radiation in a sample results in the generation of an acoustic wave. The acoustic wave can be detected by using a sensitive microphone. The intensity of the acoustic signal generated by the photoacoustic effect is proportional to the incident light power, absorbing sample concentration and the absorption coefficient of the target gas species.

A common approach to detect photoacoustic signal in traditional PAS is to use a resonant acoustic cell with a sensitive microphone [14-16]. Such a PAS detection scheme can be affected by environmental and sample gas flow noise since a microphone is designed for a widely flat frequency response. In addition, the resonant acoustic cell cannot be made too small because of the resonance condition for an acoustic wave. Quartz enhanced photoacoustic spectroscopy (QEPAS) is a rapidly developing, sensitive, selective spectroscopic technique for laser-based trace gas detection with a fast response time [17, 18]. QEPAS combines the main characteristics of photoacoustic spectroscopy (PAS) with the additional benefits of using a quartz tuning fork (QTF), thus achieving additional advantages which include small volume, low cost, high detection sensitivity, and in particular, immunity to ambient acoustic noise.

With a QCL as the radiation source, most of the molecular footprint region can be reached. To date, the QEPAS sensor technique has been employed to detect, monitor and quantify several molecules with well resolved rotational-vibrational lines in the mid-infrared spectral region (e.g., CO_2, CH_4, C_2H_2, C_2H_4, NO, N_2O, CO, NH_3, C_2H6, and CH_2O) [19-29].

A typical QEPAS sensor platform employs a focusing lens and a pinhole as the spatial filter. However, when the laser beam shape is not optimum, this basic spatial filter structure induces optical fringes due to spatial diffraction, which results in optical noises, thereby limits the sensor detection sensitivity. In this work, a dual filter structure has been implemented to minimize this problem. The second filter can effectively remove the fringes induced by the first filter.

The micro-resonator (mR) in an Acoustic Detection Module (ADM) plays a crucial role in QEPAS sensor technology and acts similarly to the acoustic resonator in conventional PAS. Both the dimensions and position of the mR influences the enhancement factor of the detection sensitivity. A detailed investigation of different mR configurations was performed and the optimum configuration is ~4.4 mm length, ~0.6 mm inner diameter (ID), and ~30 μm gap between tube facet and the QTF

surface [30].

This report is organized as follow: Section 2 presents atheoretical analysis of traditional PAS and QEPAS. The design considerations and implementation details of the QEPAS sensor platform are discussed in Section 3. Section 4 provides details of three measurements: SO_2, CO, and N_2O/CH_4. Section 5 summarizes the paper and outlines plans for future work.

II. Theoretical Analysis

A. Photo Acoustic Spectroscopy (PAS)

PAS is an established method of experimental physics. A common approach to detecting an acoustic signal generated by the modulated radiation from a laser in an absorbing gas utilizes an acoustic resonator filled with gas. The photoacoustic effect in gases can be divided into three main steps:

(1) localized heat release in the sample gas due to relaxation of absorbed light energy through molecular collisions;

(2) acoustic and thermal wave generation due to localized transient heating and expansion;

(3) detection of the acoustic signal in the photoacoustic cell with a microphone.

The detailed process is illustrated in Fig 1 [31]. A linear wave equation can be derived for the sound pressure:

$$\partial_t^2 p(r,t) - c^2 \nabla^2 p(r,t) = (\sigma - 1)\partial_t H(r,t) \quad (1)$$

where p, c, σ, and H are the pressure, sound velocity, the adiabatic coefficient of the gas, and the heat density deposited in the gas by light absorption, respectively.

There are two independent solutions for the equation [32]: a weakly damped propagating acoustic wave, and a heavily damped thermal wave. Normally, thermal and acoustic waves are separated in space due to different scales of wavelengths. Therefore, they can be investigated independently.

PAS is based on the detection of the acoustic signal. From equation (1), we can see that the acoustic signal depends on the deposited heat power density. Nearly all photoacoustic trace gas measurements are carried out in an enclosure, called a "PA cell". And the absorbed laser power is accumulated in the acoustic mode of the resonator for Q oscillation periods, where Q is the quality factor of the resonator. From classical oscillator theory, the effective integration time τ can be expressed as :

$$\tau = Q/(\pi f) \quad (2)$$

The acoustic signal is proportional to the effective integration time and can be described as :

$$S = c\frac{\alpha P Q}{f} \quad (3)$$

where C is constant, α is the absorption coefficient of the target species, P is the optical power, Q is the quality factor of the acoustic mode in the resonator, and f is the resonance frequency of the resonator. The Q factor is typically between 40 and 200, and f is in the range of 1000-4000 Hz. Achieving longer value of τ in a gas-filled resonator is limited by intrinsic loss related to gas viscosity and other relaxation process.

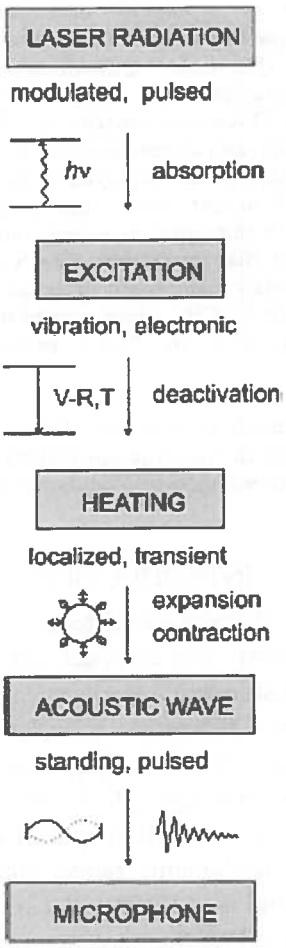

Fig 1. Schematic of the physical processes occurring after optical excitation of molecules. Modulated or pulsed laser radiation leads to the population of rotational, vibrational, and electronic states. Collisional deactivation by *R– T*, *V–R, T*, and *E–V, R, T* processes leads to localized transient heating. The resulting expansion launches standing or pulsed acoustic waves, which are detected with a microphone.

B. Quartz Enhanced Photo Acoustic Spectroscopy (QEPAS)

QEPAS is a novel approach to photoacoustic detection of trace gases, utilizing a quartz tuning fork (QTF) as a sharply resonant acoustic transducer. In the QEPAS technique, the common PAS approach is inverted and the

absorbed energy is not accumulated in the gas but in a sensitive, selective QTF. A nearly optimum commercially available QTF is shown in Fig 2 [33]. Commercial QTF typically resonate at 32,768 Hz.A typical QTF has a Q factor of ~20000 or higher when it is encapsulated in vacuum and ~8000 at normal atmospheric pressure. Due to the high Q factor, and the quadruple characteristic of the QTF,QEPAS has high immunity to background acoustic noise:

1) The ambient acoustic noise density follows a1/f dependence and is low > 10 kHz.
2) The acoustic wavelength in air is ~1 cm at 32 kHz and is longer at lower frequencies. Therefore, the sound waves emanating from a distant source will apply a force in the same direction upon the two QTF prongs positioned at a ~1mm distance, which will not cause differential signal to the QTF.
3) The high Q factor ensures the high selectivity of signals with desired frequency. The width of the QTF resonance at normal pressure is ~4 Hz which effectively exclude noises out of this range.

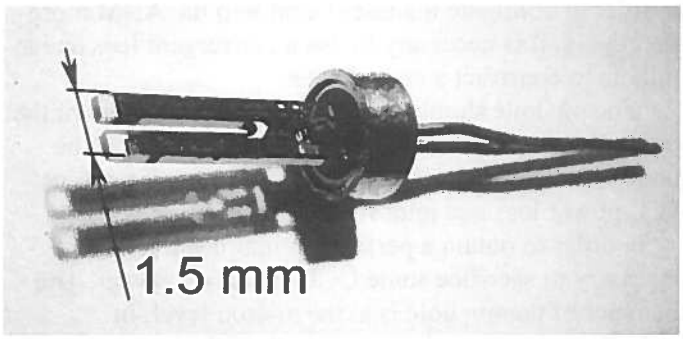

Fig. 2 Photograph of a quartz tuning fork (QTF). QTFs of this geometry are used in most QEPAS studies carried out at Rice University.

The QEPAS signal can be expressed as [34]:

$$S_{QEPAS} = C_{ADM} P_0 C Q(p)\alpha(p)\varepsilon(p) \quad (3)$$

where C_{ADM} is the Acoustic Detection Module (ADM) constant, P_0 is the incident optical power, C is the detected gas concentration, Q is the quality factor of QTF, α is the peak intensity of the 2f absorption spectrum, and ε is the conversion efficiency of the absorbed optical radiation power into acoustic energy. Q, α, and ε are pressure dependent. In addition, the peak intensity α depends on the laser wavelength modulation (WM) depth.

Assuming only collision deexcitation is considered, the conversion efficiency is related to the relaxation time τ of the target gas [35,36]:

$$\varepsilon(p) = \frac{1}{\sqrt{1+\tan^2\theta}} \quad (4)$$

$$\tan\theta = 2\pi f \tau(p) \quad (5)$$

$$\tau(p) = \frac{P_0\tau_0}{p} \quad (6)$$

where θ is the QEPAS signal phase, f is the modulation frequency, and $P_0\tau_0$ is the relaxation time constant.

There are three main noise sources: thermal noise associated with mechanical dissipation in the QTF, thermal noise of the feedback resistor, and optical noise. The QTF related thermal noise can be estimated with:

$$\sqrt{\langle V_{N-R}^2 \rangle} = R_g \sqrt{\frac{4k_B T}{R}} \sqrt{\Delta f} \quad (7)$$

$$R = \frac{1}{Q}\sqrt{\frac{L}{C}} \quad (8)$$

and the thermal noise of the feedback resistor can be estimated from Eq (9):

$$\sqrt{\langle V_{N-Rg}^2 \rangle} = \sqrt{4k_B T R_g} \sqrt{\Delta f} \quad (9)$$

where Δf is the detection bandwidth, k_B is the Boltzmann constant, T is QTF temperature, R_g is the value of the feedback resistor in a transimpedance amplifier connected to the QTF electrodes, and R, L, and C are the electrical parameters of the QTF when it is represented by the equivalent serial resonant circuit. The largest noise component usually comes from the optical noise. When the laser beam is not properly aligned, the beam will hit the QTF directly. And since the laser beam is modulated with the certain frequency which happens to be in the frequency response range of QTF, this will induce interference of the QEPAS signal.

III. Platform Design and Implementation

The schematic configuration of the QEPAS sensor platform is depicted as Fig 3. The laser beam is guided and collimated into an acoustic detection module (ADM). In the ADM, acoustic signal is transformed to an electric signal by QTF. A 2f wavelength-modulation spectroscopy (WMS) technique is adopted in this sensor platform. In this section, we describe three main components of the sensor platform: laser source, spatial filter, and the ADM. These three components significantly influence the SNR and thus the performance of the sensor platform.

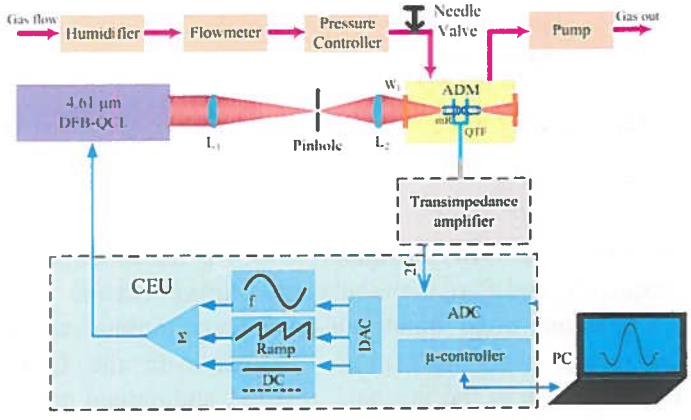

Fig 3. Schematic of a compact QCL-based QEPAS sensor platform. DFB-QCL: distributed feedback quantum cascade laser with a temperature controller and current driver; CEU: control electronics unit; QTF: quartz tuning fork; mR: micro resonator; f: laser current modulation frequency; ADC: analog-to-digital converter; DAC: digital-to-analog converter.

A. *Mid-Infrared Quantum Cascade Laser (QCL)*

In diode lasers, the reliance on the bandgap for light emission turns into a severely limiting factor at mid-infrared wavelengths, particularly in the molecular fingerprint region (3-20 μm) and beyond into the far-infrared. The QCL relies on a radically different process for light emission, which is independent of the bandgap. Instead of using opposite charge carriers in semiconductors (electrons and holes) at the bottom of their respective conduction and valence bands, QCLs use only one type of charge carrier (electrons) that undergo quantum jumps between energy levels E_n and E_{n1} to create a laser photon of frequency $(E_n - E_{n1})/h$. These energy levels do not exist naturally in the semiconductor materials of the active region but are artificially created by structuring the active region in ultra-thin layers known as quantum wells of nanometric thickness. Therefore, the QCL can operate in the mid-infrared and even in far-infrared regions with superior performance and functionality.

In this work, a HHL package thermoelectrically cooled (TEC) SO_2 distributed feedback (DFB) QCL from Alpes Lasers was employed as the spectroscopic source. The measured LIV curve and current tuning characteristics of the SO_2 QCL are illustrated in Fig 4.

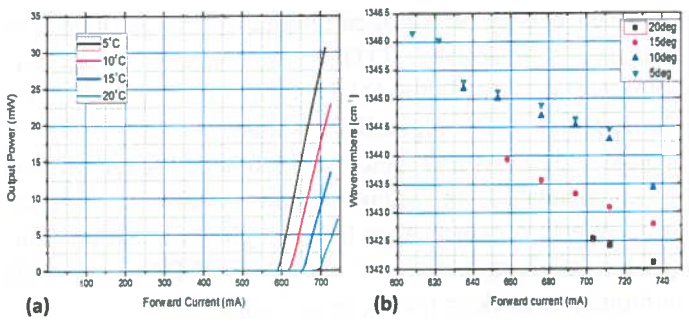

Fig 4. (a) Measured LIV curves of the 7.4 μm HHL-package TEC-DFB QCL operating at different temperatures; (b) temperature and current tuning characteristics of the 7.4 μm HHL-package TEC DFB QCL

The laser housing is mounted on an x-y-z mount. The mount is cooled by a water chiller. The TEC inside the laser housing can precisely control the operating temperature of the QCL. In order to set and monitor the temperature of the QCL, a temperature controller (TC) is connected to the QCL.

B. *Spatial Filter*

The QCL beam shape may not be perfectly Gaussian. In order to collimate the laser beam into the ADM more effectively, it is necessary to use a convergent lens and a pinhole to construct a spatial filter.

The pin hole should be placed at the focal point of the lens and with proper diameter so that the beam can be made exactly circular. Incorrect position or size causes QCL power loss and undesirable optical fringes.

, In order to obtain a perfect circular beam it is necessary to sacrifice some QCL excitation power. The diameter of the pin hole is at the micron level. In mid-infrared region, the wavelength of the laser source is also at micron level. Therefore, diffraction effects occur when the beam passes through the pin hole, In this work, a novel dual filter structure is proposed to address this problem. Instead of the basic filter, a dual filter structure was employed to eliminate the optical fringes induced by the first spatial filter. The basic filter structure and the dual filter structure are shown in Fig 5.

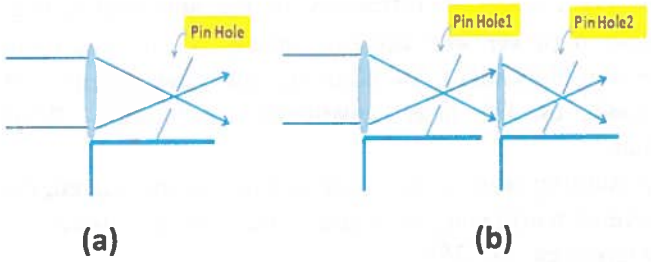

Fig 5. (a) scheme of basic filter structure: consists of one focal lens and one pinhole; (b) scheme of the dual filter structure: the second filter can effectively remove the fringes induced by the first filter.

In the dual filter structure, the position and focal length of the second lens, the position and size of the second pin hole all need to be accurate. This places more severe requirements for optical alignment and causes significant loss of the QCL power.

C. *Acoustic Detection Module (ADM)*

A typical ADM for the QEPAS-based sensor platform incorporates a QTF, two micro resonator (mR) tubes, and an enclosure that allows operation at an optimized pressure determined for a given target trace gas mixture. The design and structure of an ADM is depicted in Fig 6 [37]. The enclosure consists of an inlet and outlet connection for gas tubes and two AR coated ZnSe windows (4-12 μm transmission range) attached to the front and back of the enclosure with a total volume of <5 cm^3. The two optical windows of the enclosure are tilted so the laser beam will not reflect back and forth between the optical windows and the collimating lens. The QTF was located between the two mR tubes to detect the acoustic waves excited in the gas contained inside the mR. A charge deformation of the QTF prongs due to the piezoelectric effect produces a small current or voltage on electrodes deposited on the QTF surfaces. Subsequently, this QTF electric signal was detected using an ultra-low noise transimpedance preamplifier with a 10 MΩ feedback resistor R_g located close to the ADM. Both the QTF and the mR were attached to a metallic mount using a low vapor pressure epoxy.

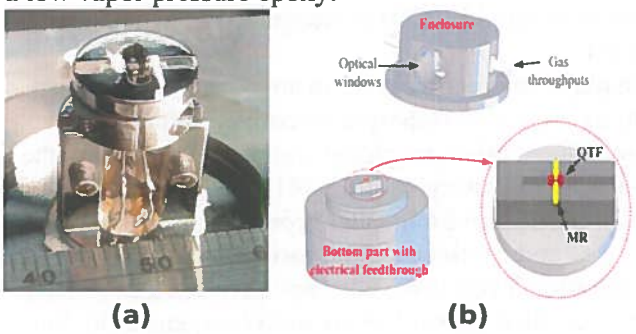

Fig 6. (a) Scheme of QTF and mR; (b) Sketch of QEPAS cell. QTF: Quartz Tuning Fork; MR: micro-resonator

The mR is important since it significantly enhances the QEPAS signal. In this design, the mR consists of two metallic tubes, and the QTF is positioned between the tubes. It is necessary to collimate the QCL beam along the two tubes and pass the gap between two prongs of QTF. The optimum condition is that the beam waist is located between the two QTF prongs, as shown in Fig 7.

Therefore, we can obtain the highest power density between the two prongs of QTF as well as avoid the QCL beam hitting the QTF.

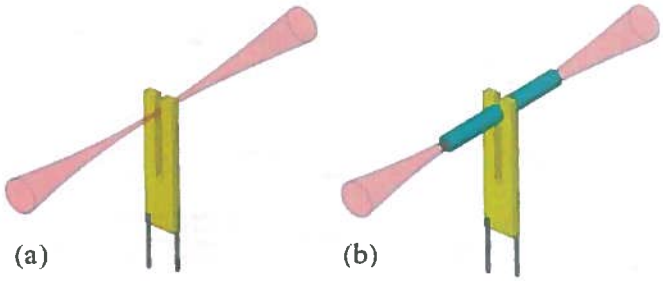

Fig 7. QTF based spectrophones: (a) simplest configuration, (b) improved configuration with an acoustic resonator formed by two pieces of rigid tubing. The beam waist should be exactly between the two prongs of QTF. QTF: Quartz Tuning Fork

Any contact between the beam and the mR tubes will result in optical noise. Shorter mR tubes with larger inner diameter are advantageous in facilitating optical alignment of the laser beam with the mR and QTF. However, the enhancement factor for QEPAS decreases when the inner diameter is too large. In addition, the length of mR is also important. Analysis of the optimum mR tube size was performed based on standing wave theory: if we assume that the two parts of the mR (left and right tubes) can be considered as a single tube, neglecting the gap and QTF between them, then each tube should be cut to the $l \approx \lambda_S/4$ length, where λ_S is the sound wavelength; if we consider the two parts of mR to be independent tubes, then each tube should be $\lambda_S/2$ length. Detailed studies [38] show that the optimum length is actually between $\lambda_S/4$ and $\lambda_S/2$ because of the interaction of two resonator tubes and acoustic coupling to the QTF. The gap size between the QTF and the mR tubes is another parameter which has a significant effect on the sensor performance. Fig 8 displays the SNR comparison for several mR tube configurations and different gaps [39]. The mR tubes with l = 4.4 mm, ID = 0.6 mm, and gap = 30 μm achieved the optimum SNR.

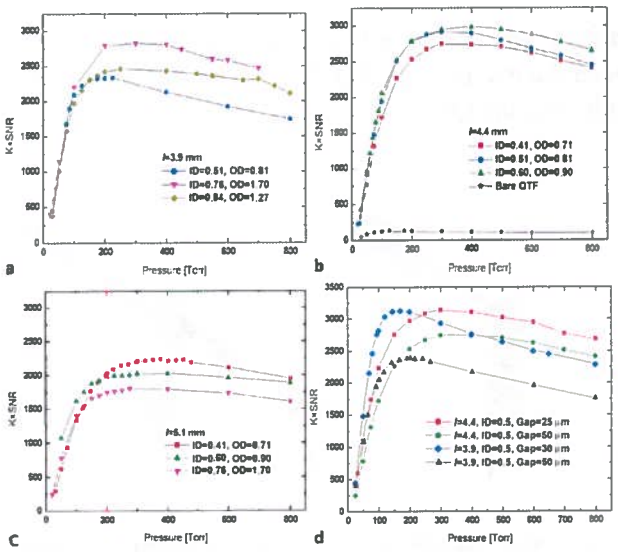

Fig 8. Signal-to-noise ratio as a function of the pressures for different QEPAS micro-resonator (mR) configurations. *l*: length of each mR tube; ID, OD: inner and outer diameter of the tube in mm: (**a**) 3.9 mm long tubes with 50μm gap, (**b**) 4.4 mm long tubes with 50μm gap and bare QTF, (**c**) 5.1 mm long tubes with 50μm gap; (**d**) Signal-to-noise ratio as a function of gas pressure for 25 μm, 30 μm and 50 μm gaps between the tube facets and the QTF surface.

IV. Platform Demonstration

In this section, we describe three demonstrations of the designed QCL-based QEPAS sensor platform: SO_2, CO , and N_2O/CH_4 measurements. In the SO_2 measurement, the dual filter structure was tested for the first time. The CO demonstration used the standard measurement process. The N_2O/CH_4 measurement demonstrates the potential of this platform to measure multiple gases simultaneously.

A. SO_2 Measurement

Sulfur dioxide (SO_2) is a major air pollutant and has significant impact on human health. Sulfur dioxide emission is a precursor to acid rain and atmospheric particulates. SO2 plays an important role in combustion processes. Therefore the capability of detecting and quantifying SO_2 is significant.

In the SO_2 measurement, we also demonstrated the newly proposed dual filter structure. In order to show the potential for the newly proposed structure, we used a laser with limited performance in this demonstration. The HHL packaged Alpes SO_2 DFB QCL has a bat-like beam shape and low power. Fig 9 shows the initial beam shape, the beam shape after the spatial filter , and the beam shape after the dual spatial filter. The dual filter structure effectively removed the fringes around the main beam spot which reduced the optical noise dramatically.

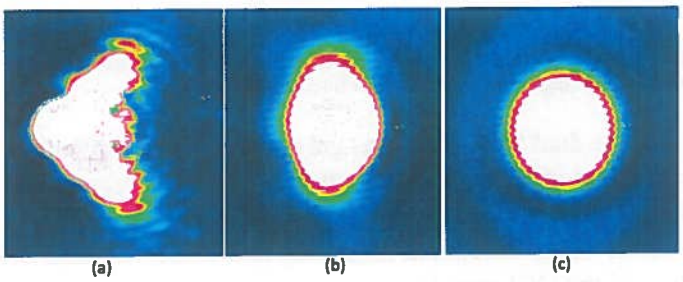

Fig 9. (a) Beam shape of Alpes SO_2 TEC-DFB QCL; (b) beam shape after spatial filter ; (c) beam shape after the dual filter structure.

Spectral scans of a moisturized 10ppm SO_2 sample and a moisturized nitrogen sample at 200Torr are depicted in Fig 10. After effective suppression of the optical noise, we obtain a QEPAS signal with the above mentioned ~10 mW QCL.

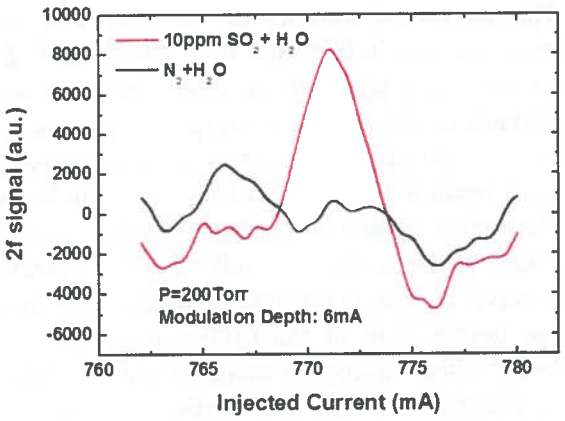

Fig 10.QEPAS spectrum of a moisturized 10 ppm SO_2 sample and moisturized nitrogen sample.

B. CO Measurement

Carbon monoxide (CO) is recognized as a major air pollutant
which plays an important role in atmospheric chemistry due to its impact on tropospheric ozone formation [40] and an indirect effect on global warming by reducing the abundance of hydroxyl radicals [41]. The current method used by the US Environmental Protection Agency for automated and continuous monitoring of ambient CO concentration levels is the nondispersive infrared (NDIR) technique with a typical 1 ppmv detection sensitivity limit, a ~30 sec response time and sample pretreatment [42]. The availability of a compact CO sensor with ppbv-level detection sensitivity and fast response will allow effective monitoring and quantification of CO urban and industrial emissions. With the compact QCL-based QEPAS sensor platform, we can realize sensitive, selective, and noise-immune detection at ppbv concentration levels.

Carbon monoxide detection in the mid-IR region was demonstrated with our designed QEPAS sensor platform in this work. A , widely tunable TEC QCL at a

wavelength of 4.6 μm [reference] was employed as the radiation source. The measured LIV curves and laser tuning characteristics are shown in Fig 11. Since CO has a slow vibrational-translational (V-T) energy relaxation process, water vapor (2.6% H_2O) as the catalyst was added to enhance the QEPAS CO signal. A water chiller was connected to the laser housing in order to dissipate the heat produced by the TEC inside the HHL packaged QCL. The laser temperature and current were controlled by the Control Electronics Unit (CEU) and set to 15 °C and 795 mA, respectively. A LabView program was used to determine critical QTF parameters such as the resonance frequency f_0, Q-factor, and dynamic resistance R, before starting measurements. In order to perform 2f-WMS, the QCL frequency was scanned across the selected R(6) CO absorption line (shown in Fig 11(c)) by applying a slow saw-tooth ramp to the QCL. Furthermore, a sinusoidal signal at $f_0/2$ was superimposed on the saw-tooth ramp in order to modulate the scanning current. Both the scanning current and the modulation signal were generated by the CEU.

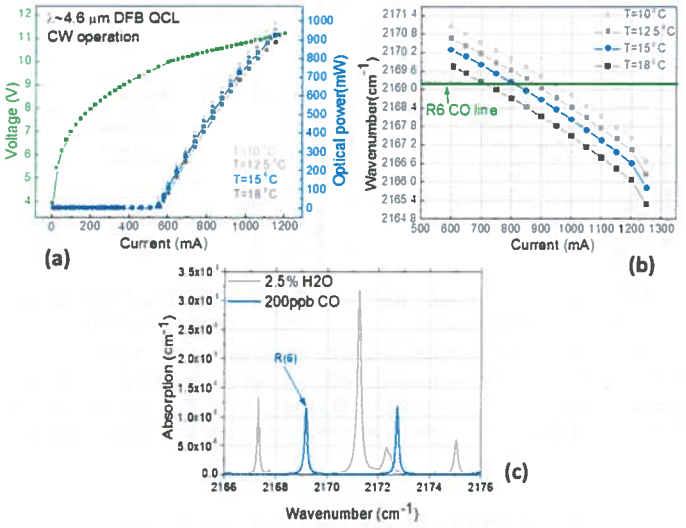

Fig 11. (a) Measured LIV curves of the 4.6μm continuous wave DFB QCL operating at different temperatures; (b) temperature and current tuning characteristics of the 4.6μm continuous wave DFB QCL operating at different temperatures; (c) HITRAN absorption spectra of 200 ppb CO, and 2% water simulated for a 760 Torr gas pressure and a 1 m effective optical path length

A Nafion humidifier and a hygrometer were connected to the ADM in order to add water vapor to the target gas mixture and monitor its water content, respectively. A needle valve was employed to set the gas flow to a constant rate of 100 scc/min. A pressure controller and an oil free diaphragm vacuum pump were placed after the ADM to control and maintain the CO sensor pressure. In this work, the sensor operated at a pressure of 760 Torr. The CO QEPAS spectra of the *R(6)* line acquired at 760 Torr for a dry and moisturized 5 ppmv CO:N2 mixture as well as pure nitrogen (background noise) are shown in Fig. 12(a)(b). From spectral scans of different CO concentrations, we obtained a linear dependence between signal amplitude and CO concentration, as depicted in Fig 12(c). With this linear fit, the gas concentration can be derived from the QEPAS signal intensity. The detection limit can be estimated by expanding the linear fit line to the limit of noise level. A 1σ minimum detection limit of 2ppbv was obtained at atmospheric pressure with 1 second sampling time.

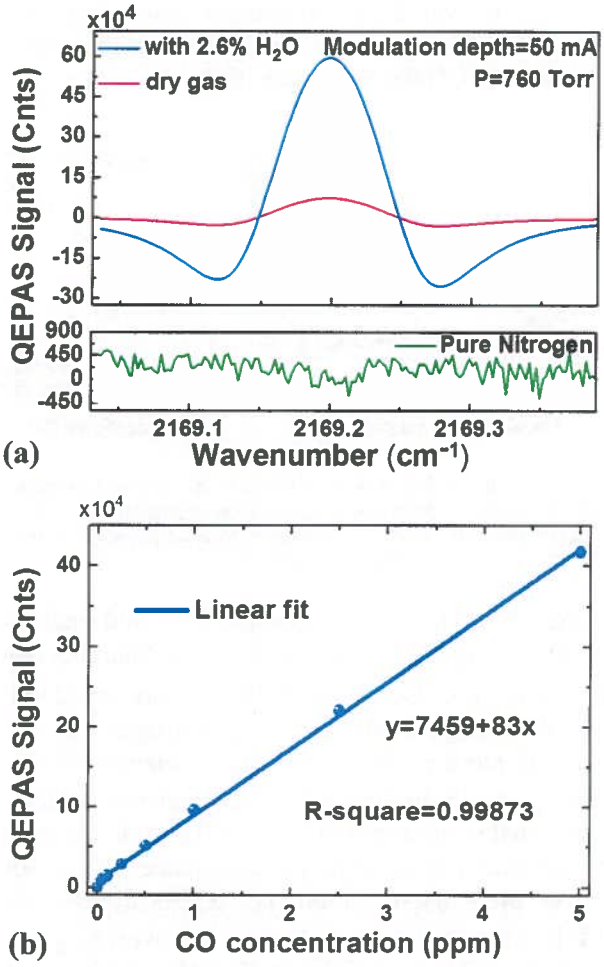

Fig 12. (a) QEPAS spectrum of a dry and moisturized 5ppmv CO:N_2 mixture at the R(6) absorption line as well as pure nitrogen; (b) experimental results and linear fit between CO concentration and QEPAS signal. The QEPAS signal is recorded in terms of internal CEU units

In order to yield the highest 2f QEPAS signal, the modulation depth must match the pressure-dependent absorption line width. The CO QEPAS signal dependence of current modulation depth at different pressures is depicted in Fig 13(a). The addition of 2.6 % water results in a ~8 times signal enhancement, which confirmed that the presence of water can significantly improve the CO V-T relaxation rate. The effect of the water present in the CO mixture was investigated by varying its concentration from 0 to 2.6% by volume at a total gas pressure of 760

Torr. The measured QEPAS signal as a function of the water concentration is depicted in Fig 13(b).The volume percent of the maximum amount of water vapor that can be added to the gas mixture is 2.6% due to the humidifier performance. However, based on the trend of the curve shown in Fig. 13(b), the QEPAS signal is expected to reach an optimum level for a much higher water vapor concentration than 2.6 %. In fact, such a behavior can be beneficial for breath diagnostics since the water concentration in the exhaled breath is at a ~5 % concentration level. In environmental monitoring, the addition of >2 % water to the analyzed mixture is helpful to improve the CO detection sensitivity.

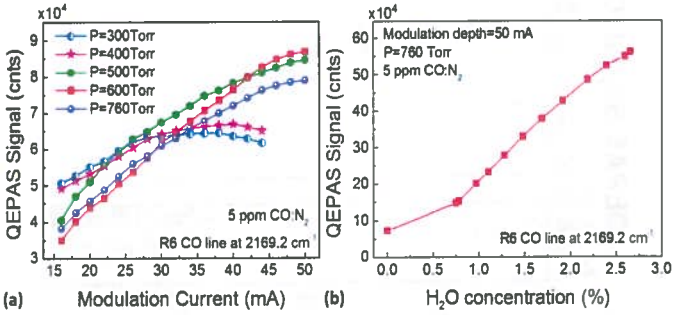

Fig 13. (a) QEPAS signal of the peak CO R(6) absorptionas a function of wavelength modulation depth (current modulation amplitude) acquired at different pressures; (b) QEPAS signal obtained from a 5 ppmv CO:N_2 mixture at 760 Torr as a function of water concentration.

In order to characterize long-term drifts and establish signal averaging limits, the results of the Allan deviation $\sqrt{\langle \sigma_A^2 \rangle}$ in terms of CO concentration are presented in Fig. 14. For this analysis, pure carrier gas nitrogen was introduced into the ADM. The Allan deviation at the beginning closely follows a $1/\sqrt{t}$ dependence, which indicates that white Johnson noise of the QTF remains the dominant source of noise for time sequences of 1 to 300 s. However, the Allan deviation experiences a sensitivity drift following the $\sqrt{t}$ dependence when averaging exceeds 600 s. Thus a stability period of 300–600 s and an optimal detection sensitivity of ~350 ppt can be realized.

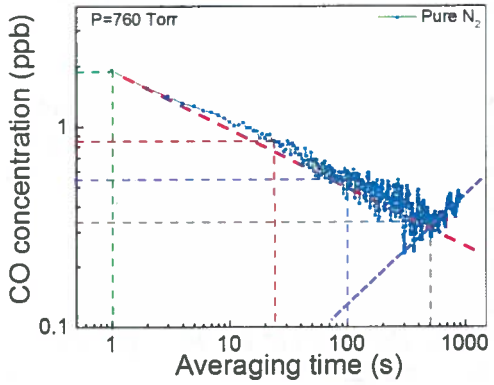

Fig 14. Allan deviation as a function of the data averaging period. Dashed red line follows a $1/\sqrt{t}$ slope. Dotted purple line follows a $\sqrt{t}$ slope.

C. N_2O/CH_4 Measurements

The QCL-based QEPAS sensor platform is wavelength independent and is therefore applicable in spectroscopic measurements ranging from the near infrared to the mid infrared. This makes it possible for the QEPAS sensor platform to realize multiple gas species detection with widely tunable QCL as the radiation source. In this work, a 7.83 μm distributed feedback (DFB) QCL from AdTech Optics (HHL-12-25) was employed as the laser source for the QEPAS sensor platform. This QCL can be tuned across the wavenumber range between 1272.5 cm^{-1} to 1276.5 cm^{-1} with a output power of >100 mW. This QCL can access several strong and interference-free absorption lines of N_2O and CH_4, as shown in Fig 15(a). Therefore, it is possible to detect N_2O and CH_4 simultaneously with this laser source. The QEPAS spectral scans of a moisturized 1.8 ppmv N_2O sample and a moisturized ambient air sample are depicted in Fig 15(b). The detection limit of N_2O/CH_4 can reach 16 ppbv for N_2O and 60 ppbv for CH_4, respectively.

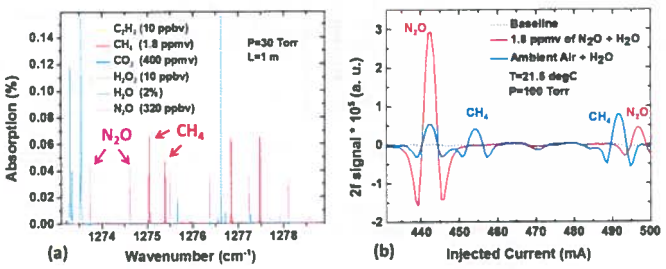

Fig 15. (a) HITRAN absorption spectra of 320 ppb N_2O, 1.8 ppm CH_4, 10 ppb C_2H_2, 400ppm CO_2, 10 ppb H_2O_2, and 2% water simulated for a 30 Torr gas pressure and a 1 m effective optical path length; (b) QEPAS spectral scans of moisturized 1.8 ppmV N_2O and moisturized ambient air at 100 Torr pressure

V. Conclusions and Future Work

In this work, a QCL-based QEPAS sensor platform was designed, assembled and its performance was evaluated. The characteristics of the QCL, spatial filter, and ADM were discussed. The configuration of the micro-resonator in the ADM significantly influences sensor performance which must be taken into account in its design. Measurements of SO_2, CO, N_2O/CH_4 were performed to demonstrate the design of the QEPAS sensor platform. These measurements confirmed the potential of a QEPAS sensor platform for ppbv level trace gas detection as well as simultaneous detection of multiple gas species. The CO measurement can reach a 1σ detection limit of 2ppbv with 1 second time resolution. The N_2O/CH_4 measurement can obtain 16ppbv detection limit for N_2O and 60ppbv detection limit for CH_4, respectively. A novel

dual filter structure was demonstrated in the SO_2 measurement to minimize the optical noise due to a non-optimum QCL beam shape. The availability of an optimized HHL-packaged 7.73 μm DFB QCL from Corning Inc. will allow us to perform detection of hydrogen peroxide (H_2O_2) which is an important greenhouse gas in an urban/industrial environment. General methods of detecting H2O2 include infrared/Raman spectroscopy, mass spectrometry, electrochemical method, colorimetric and fluorimetric detection [43]. However, these methods require costly and bulky equipment requiring lengthy sample preparation, have limited selectivity and detection sensitivity. Since the QEPAS sensor platform is capable of compactness, high selectivity, high sensitivity, and fast response time, it is a very promising technique for H_2O_2 detection.

REFERENCES

[1] R.F. Curl, F. Capasso, C. Gmachl, A.A. Kosterev, B. McManus, R. Lewicki, M. Pusharsky, G. Wysocki, F.K. Tittel, "Quantum cascade lasers in chemical physics." Chem. Phys. Lett. 487, 1 (2010)

[2] M. Troccoli, L. Diehl, D.P. Bour, S.W. Corzine, N. Yu, C.Y.Wang, M.A.Belkin, G. Hofler, R. Lewicki,G.Wysocki, F.K. Tittel, F. Capasso, "High-Performance Quantum Cascade Lasers Grown by Metal-Organic Vapor Phase Epitaxy and Their Applications to Trace Gas Sensing." J. Lightwave Technol. 26, 3534 (2008)

[3] A.A. Kosterev, G. Wysocki, Y.A. Bakhirkin, S. So, R. Lewicki, F.K. Tittel, R.F. Curl, "Application of quantum cascade lasers to trace gas analysis M. Sigrist (Ed.) Selected papers from the International Conference on Tunable Lasers and Fundamental Laser Spectroscopy."Appl. Phys. B 90, 165 (2008)

[4] A.A. Kosterev, F.K. Tittel, G. Bearman, "Advanced quartz-enhanced photoacoustic trace gas sensor for early fire detection."in Proceedings of the 2008 Int. Conference on Environmental Systems, Published by SAE as MS 08ICES-0031 (2008)

[5] J.S. Pilgrim, J. Kutzner, W.R. Wood, "High-performance optical contaminant monitor for spacecraft and habitats." in Proceedings of the 2007 Int. Conference on Environmental Systems, Published by SAE as MS 2007-01-3152 (2007)

[6] M.R. McCurdy, Y.A. Bakhirkin, G.Wysocki, R. Lewicki, F.K. Tittel, "Recent advances of laser-spectroscopy-based techniques for applications inbreath analysis." J. Breath Res.1, 014001 (2007)

[7] G. Wysocki, Y.A. Bakhirkin, S. So, F.K. Tittel, C.J. Hill, R.Q. Yang, M.P. Fraser, "Dual interband cascade laser based trace-gas sensor for environmental monitoring." Appl. Opt. 46, 8202 (2007)

[8] J.S. Li, X.M. Gao, L. Fang, W.J. Zhang, H. Cha, Opt. Laser Technol.39, 1144 (2007)

[9] A. Miklos, P. Hess, Z. Bozoki, "Application of acoustic resonator in photoacoustic trace gas analysis and metrology." Rev. Sci. Instrum. 72, 1937 (2001)

[10] M.G. Da Silva, H. Vargas, A. Miklos, P. Hess, "Photoacoustic detection of ozone using a quantum cascade laser." Appl. Phys. B 78, 677 (2004)

[11] M.A. Gondal, "Laser photoacoustic spectrometer for remote monitoring of atmospheric pollutants." Appl. Opt. 36, 3195 (1997)

[12] S. Schilt, L. Thevenaz, M. Nikles, L. Emmenegger, C. Huglin, Spectrochim. Acta A 60, 3259 (2004)

[13] A.G. Bell, Am. J. Sci. 20, 305 (1880)

[14] J.S. Li, X.M. Gao,W.Z. Li, Z.S. Cao, L.H. Deng,W.X. Zhao,M.Q. Huang, W.J. Zhang, Spectrochim. Acta A 64, 338 (2005)

[15] F.G.C. Bijnen, J. Reuss, F.J.M. Harren, Rev. Sci. Instrum. 67, 2914 (1996)

[16] A. Petzold, R. Niessner, Appl. Phys. Lett. 66, 1285 (1995)

[17] A.A. Kosterev, F.K. Tittel, D.V. Serebryakov, A.L. Malinovsky, I.V. Morozov, Rev. Sci. Instrum. 76, 043105 (2005)

[18] A.A. Kosterev, Y.A. Bakhirkin, R.F. Curl, F.K. Tittel, "Quartz-enhanced photoacoustic spectroscopy," Opt. Lett. 27, 1902 (2002)

[19] A.A. Kosterev, F.K. Tittel, "Ammonia monitoring at trace level using photoacoustic spectroscopy in industrial and environmental applications." Appl. Opt. 43, 6213 (2004)

[20] L. Dong, A.A. Kosterev, D. Thomazy, F.K. Tittel, "Compact Portable QEPAS Multi-gas Sensor." Proc. SPIE 7945, 50R-1 (2011)

[21] D.Weidmann, A. A Kosterev, F. K Tittel, N. Ryan, D. McDonald, "Monitoring of ethylene by a pulsed quantum cascade laser." Opt. Lett. 29, 1837 (2004)

[22] A.A. Kosterev, L. Dong, D. Thomazy, F.K. Tittel, S. Overby, "QEPAS for chemical analysis of multi-component gas mixtures." Appl. Phys. B, Lasers Opt. 101, 649 (2010)

[23] S. Schilt, Anatoliy A. Kosterev, Frank K. Tittel, "Performance evaluation of a near infrared QEPAS based ethylene sensor." Appl. Phys. B 95, 813 (2009))

[24] L. Dong, V. Spagnolo, R. Lewicki, F.K. Tittel, "Ppb-level detection of nitric oxide using an external cavity quantum cascade laser based QEPAS sensor." Opt. Express 19, 24037 (2011)

[25] V. Spagnolo, A.A. Kosterev, L. Dong, R. Lewicki, F.K. Tittel, "NO trace gas sensor based on quartz enhanced photoacoustic spectroscopy and external cavity quantum cascade laser." Appl. Phys. B, Lasers Opt. 100, 125 (2010)

[26] A. A Kosterev, Y.A. Bakhirkin, F.K. Tittel, "Ultrasensitive gas detection by quartz-enhanced photoacoustic spectroscopy in the fundamental molecular absorption bands region." Appl. Phys. B 80, 133 (2005)

[27] R. Lewicki, A.A. Kosterev, D.M. Thomazy, T.H. Risby, S. Solga, T.B. Schwartz, F.K. Tittel, "Real time ammonia detection in exhaled human breath using a distributed feedback quantum cascade laser based sensor." Proc. SPIE 7945, 50K-2 (2011)

[28] A.K. Ngai, S.T. Persijni, D. Lindsay, Anatoliy A. Kosterev, P. Gross, C.J. Lee, C.M. Cristescu, Frank K. Tittel, K.J. Boller, F.J. Harren, "Continuous Wave Optical Parametric Oscillator for Quartz-Enhanced Photoacoustic Trace Gas Sensing." Appl. Phys. B 89, 123 (2007)

[29] M. Horstjann, Y. A Bakhirkin, A.A. Kosterev, R.F. Curl, F.K. Tittel, C.M. Wong, C.J. Hill, R.Q. Yang, "Formaldehyde sensor using interband cascade laser based quartz-enhanced photoacoustic spectroscopy." Appl. Phys. B 79, 799 (2004)

[30] Lei Dong, Anatoliy A. Kosterev, David Thomazy, Frank K. Tittel, "QEPAS spectrophones: design, optimization, and performance." Appl Phys B 100: 627-635 (2010)

[31] Andra´s Miklo´s, Peter Hess, Zolta´n Bozo´ ki, "Application of acoustic resonators in photoacoustic trace gas analysis and metrology", Rev. Sci. Instrum. 72, 1937(2001)

[32] P. M. Morse and K. U. Ingard, Theoretical Acoustics (Princeton University Press, Princeton, NJ, 1986).

[33] F.K. Tittel, R.F. Curl, L. Dong, and et al, "Recent Advances in Infrared Semiconductor Laser based Chemical Sensing Technologies.", Springer, Proc. of NATO Advanced Research Workshop, Marmaris, Turkey, 3-6 Nov. 2009: 165-173 (2011)

[34] A.A. Kosterev, Y.A. Bakhirkin, F.K. Tittel, S. Mcwhorter, B. Ashcraft, "QEPAS methane sensor performance for humidified gases." Appl. Phys. B, Lasers Opt. 92, 103 (2008)

[35] T.L. Cottrell, J.C. McCoubrey, Molecular Energy Transfer in Gases (Butterworths, London, 1961)

[36] Anatoliy A Kosterev, T S Moseley, Frank K Tittel, "Impact of humidity on quartz-enhanced photoacoustic spectroscopy based detection of HCN." Appl. Phys. B. 85: 295-300 (2006)

[37] K Liu, J Li, L Wang, T Tang, W Zhang, Xiaoming Gao, Weidong Chen, Frank K Tittel, "Trace gas sensor based on quartz tuning fork enhanced laser photoacoustic spectroscopy." *Applied Physics B* **94**: 527-533 (2009)

[38] D.V. Serebryakov, I.V. Morozov, A.A. Kosterev, V.S. Letokhov, "Laser microphotoacoustic sensor of ammonia traces in the atmosphere." Quantum Electron. 40, 167 (2010)

[39] Lei Dong, Anatoliy A. Kosterev, David Thomazy, Frank K. Tittel, "QEPAS spectrophones: design, optimization, and performance." *Appl Phys B* **100**: 627-635 (2010)

[40] J.A. Logan, M.J. Prather, S.C.Wofsy, M.B. McElroy, "Tropospheric Chemistry: A Global Perspective." J. Geophys. Res. 86, 7210 (1981)

[41] M.A.K. Khalil, R.A. Rasmussen, "Carbon Monoxide in the Earth's Atmosphere: Increasing Trend." Science 224, 54 (1984)

[42] United states environmental protection agency, EPA 600/P-99/001F (2000)

[43] J. Zheng, Y. Yan, X. Wang, and et al, "Hydrogen Peroxide Vapor Sensing with Organic Core/Sheath Nanowire Optical Waveguides," Adv. Mater. 24, OP194-OP199 (2012)